

Artificial neural network based modeling for the prediction of yield and surface area of activated carbon from biomass

Mochen Liao, Stephen S Kelley, and Yuan Yao, Department of Forest Biomaterials, North Carolina State University, Raleigh, NC, USA

Received November 26, 2018; revised January 30, 2019; accepted January 31, 2019

View online at Wiley Online Library (wileyonlinelibrary.com);

DOI: [10.1002/bbb.1991](https://doi.org/10.1002/bbb.1991); *Biofuels. Bioprod. Bioref.* (2019)



Abstract. Activated carbon (AC) is an adsorbent material with broad industrial applications. Understanding and predicting the yield and quality of AC produced from different feedstock is critical for biomass screening and process design. In this study, multi-layer feedforward artificial neural network (ANN) models were developed to predict the total yield and surface area of AC produced from various biomass feedstock using pyrolysis and steam activation. In total, 168 data samples identified from experiments in literature were used to train, validate, and test the ANN models. The trained ANN models showed high accuracy ($R^2 > 0.9$) and demonstrated good alignment with the independent experimental data. The impacts of using datasets based on different biomass characterization methods (i.e., ultimate analysis and proximate analysis) were evaluated and compared. Finally, a contribution analysis was conducted to understand the impact of different process factors on AC yield and surface area. © 2019 Society of Chemical Industry and John Wiley & Sons, Ltd

Supporting information may be found in the online version of this article.

Keywords: artificial neural network; steam activation; activated carbon; lignocellulosic biomass

Introduction

Activated carbon (AC) is an adsorbent material with high porosity, large adsorption capacity, and superior surface reactivity.¹ It has been widely used as an adsorbent and a catalyst in the manufacturing, pharmaceutical, water treatment, and agricultural sectors.^{2,3} Activated carbon can be produced from a variety of feedstocks such as coal, petroleum residues, woods,

agricultural residues, and other carbonaceous resources.⁴ Using renewable feedstock such as biomass and agricultural / industrial byproducts (e.g., biochar) has gained increasing attention for its potential to reduce life cycle environmental footprints, and enhance the efficiency of natural resource utilization.⁴

There are currently two general methods to produce AC from biomass — chemical activation and physical activation. Steam activation, a typical type of physical activation,

Correspondence to: Yuan Yao, Department of Forest Biomaterials, North Carolina State University, Raleigh, NC, USA 27695.
E-mail: Yuan_Yao@ncsu.edu

has been commercialized to produce AC for environmental applications.⁵ The quality and physicochemical properties of AC produced by steam activation are driven by many factors such as feedstock quality and composition, steam-to-carbon ratio, and operational conditions (e.g., time, temperature, and oxidative atmosphere) of the carbonization and activation processes.^{6,7} To produce high-quality AC products, it is critical to understand the effects of various biomass feedstock and process parameters. Furthermore, given a large number of biomass candidates, there is a need for decision-support tools that can be used by scientists, engineers, and industry to screen different kinds of biomass and to tailor the initial process design strategies for specific feedstock candidates.

Previous studies indicated that a high ash content in the feedstock leads to low adsorption capacity for AC.^{8,9} Aworn *et al.*¹⁰ tried to optimize the Brunauer–Emmett–Teller (BET) surface area of AC from agricultural waste at different activation temperature. They found that optimal activation temperature depends on the type of biomass feedstock and its composition – in particular ash content.¹⁰ The effects of operational conditions on AC production have also been studied by separately examining the initial carbonization and subsequent activation steps. In the carbonization step, previous studies indicated that temperature and residence time are key parameters affecting the yield and quality of AC product. For example, Li *et al.*¹¹ investigated AC produced from coconut shell and found that higher carbonization temperatures resulted in lower yield and a higher BET surface area of AC. Regarding the activation step, most previous studies focused on the impact of activation temperature and time, and steam to biochar ratio (the total mass of steam in the activation step divided by the mass of biochar). Chen *et al.*¹² found that the yield of AC from pine nut shells decreased as the activation temperature increased from 750 to 950 °C. Similar trends have been reported in other studies using *Sicyos angulatus L.* and bamboo wastes as feedstock.^{13,14} Another study indicated that increasing steam-to-biochar ratio decreases AC yield.¹⁵

A few studies have tried to develop predictive models by statistically analyzing the relationships between process conditions and the quality of final AC products. Azargohar *et al.* used a central composite design (CCD) to understand the impacts of activation temperature, activation time, and steam-to-biochar ratio on the yield and BET surface area of AC produced by steam activation of spruce wood and lignite coal.^{16,17} Other studies used CCD to optimize ACs for methane adsorption,¹⁸ chemical oxygen demand removal,¹⁹ and iodine number.²⁰ Most previous

studies have focused on analyzing operating parameters of steam activation process, while fewer have conducted a systematic evaluation of the biomass feedstock type and composition. Jiang *et al.*²¹ used different machine learning approaches such as linear regression, support vector regression, and random forest regression, to predict the methylene blue number and iodine number of the straw-based AC product. Their study included the composition data of three different types of straw as well as both carbonization and activation processes.²¹ However, none of this prior work tried to evaluate or predict the interactions between a wide variety of biomass feedstocks and a wide variety of carbonization and activation conditions.

This work fills gaps in the prior work, and explicitly addresses the impacts of the interaction between the biomass source and the activation process on the final AC properties using artificial neural networks (ANN). ANN is a data-driven approach that can reveal complex relationships between multiple inputs and outputs without the need for a mathematical description of the phenomena.²² Unlike a programmed model, an ANN model is a trained system that has adaptability and improved accuracy with updated data.²³ It has been applied to predict the process parameters of biomass conversion such as oil extraction yields,²⁴ kinetic parameters of pyrolysis,²² and selectivity of pyrolysis products.²⁵ However, to the best of our knowledge, ANN has not been applied to the steam-activation process to predict AC yield and surface area. With the ability to unveil complex relationships between input and output variables, ANN has great potential for predicting the quantity and quality of AC products derived from different biomass feedstock.

In this study, ANNs are developed to predict the total yield and BET surface area of AC production. The ANN model presented in this study can be used for early-stage screening of biomass feedstock before intensive investment in research and development (R&D). It can also be used by a broad range of stakeholders such as scientists, engineers, and project managers to enhance experimental and process design. In addition, the predicted data (e.g., AC yield) from ANN models can be used in the process simulation (e.g., Aspen Plus simulation) for AC production using different biomass feedstock, where AC yield is a key input data.²⁶

Material and methods

In this study, two multilayer feedforward ANNs were developed to predict the total yield (Y_T) and BET surface area (S_{BET}) of AC production. The Y_T and S_{BET} are com-

monly used to indicate the performance of AC production due to their dominant impact on the production costs and performance of ACs.^{3,27} In feedforward ANNs, the outputs of one layer of neurons are fed into the next layers of neurons without any backward connection.²⁸ This type of ANN has been applied to many chemical engineering problems.²⁹

Using the common definition from the literature, Y_T is defined as the dry weight of AC product divided by the dry weight of the feedstock, as shown in Eqn (1). S_{BET} is determined by the BET method, which is a common method for measuring the surface characteristics of porous solids.³⁰

$$Y_T = \frac{\text{mass of AC product}}{\text{mass of feedstock}} \times 100\% \quad (1)$$

The ANN models in this work were trained using 11 input parameters, including six related to feedstock composition (i.e., carbon content, hydrogen content, and oxygen content from ultimate analysis; fixed carbon, volatile matter, and ash content from proximate analysis), two related to carbonization conditions (i.e., carbonization temperature and time), and three related to activation conditions (i.e., activation temperature, time, and steam to biochar ratio). The input parameters were collected from 20 literature references that studied a wide variety of biomass feedstock (see Table S1 in the supplementary material for data samples).

To test the capability of the ANN models for predicting Y_T and S_{BET} across a broad range of biomass feedstock, an extra validation was performed using a relatively comprehensive set of experimental data from Chen et al.¹² The work by Chen et al.¹² used pine nut shell as a feedstock, and none of the other data sets used in the training the ANN model included pine nut shell as a feedstock. A comparison between the two alternative data sets used for model validation will be discussed in detail below. A contribution analysis was performed to understand the impacts of feedstock composition and process parameters on Y_T and S_{BET} across different biomass feedstock.

Analytical scenarios

The input data were all collected from the literature. Based on a preliminary evaluation of this data it was found that many studies did not measure both ultimate and proximate analysis. This has been attributed to the cost and complexity of the special instruments used to measure ultimate analysis, while proximate analysis is relatively easy to measure.³¹ This limitation was addressed by creating three scenarios to investigate the impacts of alternative

attributes to measure biomass characteristics on the accuracy of ANN models:

- Scenario 1: proximate analysis + carbonization conditions + activation conditions (eight input variables).
- Scenario 2: ultimate analysis + carbonization conditions + activation conditions (eight input variables).
- Scenario 3: proximate analysis + ultimate analysis + carbonization conditions + activation conditions (11 input variables).

Experimental data collection and pre-processing

To provide some level of consistency the references were screened using the following criteria:

- Biomass feedstock was identified with transparent data for elemental analysis and / or proximate analysis.
- Data on Y_T and/or S_{BET} included a clear description of the analytical method and calculation procedure.
- Specific time and temperature information on carbonization and activation processing conditions.
- Carbonization dwell times were greater than 10 min, and there was an oxygen-free atmosphere for both the carbonization and activation steps.
- Peer-reviewed journal articles in the past 20 years.

The data can be preprocessed by normalization to enhance the learning speed of ANN, as the output of ANN becomes more sensitive to variation in input values.^{32,33} In this study, the data are normalized by a linear normalization function as shown in Eqn (2).³³

$$S_{i,j} = (V_{i,j} - Min_j) / (Max_j - Min_j) \quad (2)$$

where $S_{i,j}$ is the normalized value for each data point, $V_{i,j}$ in the data sample i ($i = 168$) for parameter j ($j = 8, 8$, and 11 for input parameters in three scenarios and 2 for output parameters). Min_j and Max_j are the minimum and maximum for parameter j .

Artificial neural network

In this work, multilayer perceptron (MLP) feedforward neural networks were developed to predict Y_T and S_{BET} . A typical MLP structure consists of three types of layers³⁴: an input layer representing input variables, an output layer including output variables, and one or more connected hidden layers simulating the correlations between inputs and outputs. The structure of the ANNs developed in this study is shown in Fig. 1.

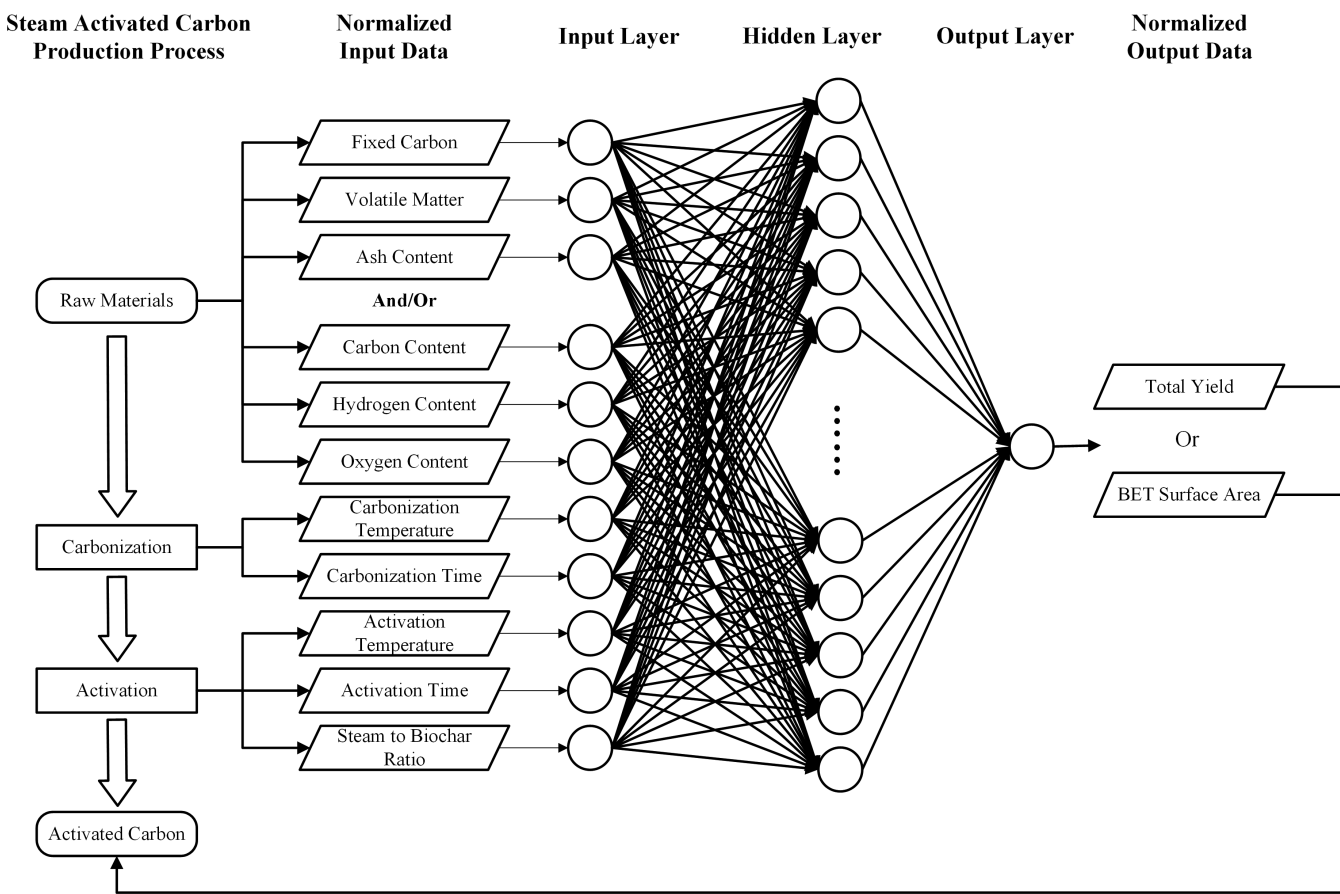


Figure 1. Schematic of ANN to predict the total yield and BET surface area of steam activated carbon.

Neurons in hidden layers connect normalized input to output data by the activation function (f_{act}) as shown in Eqn (3):

$$y_j = f_{act} \left(\sum_i w_{ij} x_i + \theta_j \right) \quad (3)$$

where x_i is the i th component of input vector; y_j is the output of j th neuron; w_{ij} is the weight from i th component of the input layer to the j th neuron in the hidden layer; θ_j is the bias of j th neuron in the hidden layer, which is summed up with other input values of j th neuron to provide an additional adjustable parameter. Equation (3) is also used for the output layer to process the data fed by hidden layers. Typically, different activation functions are selected for hidden and output layers. In this study, the tan-sigmoidal function (*tansig* as shown in Eqn (4)) was used as the activation function of hidden layer, and linear transfer function (*purelin*, as shown in Eqn (5)) was selected for the output layer. This combination was selected based on its effectiveness in previous studies.^{22,24,35–37}

$$\text{tansig}(x) = \frac{2}{1 + e^{-2x}} - 1 \quad (4)$$

$$\text{purelin}(x) = x \quad (5)$$

The number of hidden layers and the number of neurons in each hidden layer are important parameters in constructing the ANNs.³⁸ In this study, the number of hidden layers was selected to be similar to previous studies with similar data sample size.²²

The number of neurons in the hidden layer must be determined carefully. Setting the number of neurons too high may lead to overfitting, where the ANN model learns unnecessary details of training data³⁹ and then has decreased value for predicting the behavior of new samples. Setting the number of neurons too low (offsetting) may result in a failure to reach the optimal conditions and leads to ‘underfitting’ in the training process, with a subsequent decline in the quality of any future ANN-predicted data.⁴⁰

There are no standard rules for selecting suitable number of neurons in hidden layers,⁴¹ so the number of neurons is commonly determined by trial and error.⁴² In this study, two approaches are used to avoid offsetting and overfitting. First, the number of neurons (from 10 to 20) was

varied during the training, and those with reasonable combinations of computation time and high R^2 were kept (e.g. convergence in 1000 iterations with overall $R^2 > 0.9$). Then the simulation results were tested against the independent experimental data with changing input parameters (e.g., temperature changing from 750 to 950 °C) to check for overfitting. This allowed for determination of the final number of neurons for ANN models for each combination of inputs and outputs.

Training an ANN model is the process modifying the connecting weights between neurons (w_{ij}) and biases of neurons (θ_j) of ANN (Eqn (3)) according to the training data.^{42,43} Different algorithms are available to perform this training process, and back-propagation algorithm (BP) is one of the most widely used algorithms in MLP training.⁴¹ Thus, it was selected to train the ANN models developed in this work. To ensure the generalization capacity of ANN models, early stopping and regularization are common strategies used along with the training algorithm.⁴⁴ In this study, the Levenberg–Marquardt method (LM), one common early-stopping strategy, was used along with the BP algorithm. Using the combined LM-BP algorithms, the 155 of 168 member dataset was randomly partitioned into ‘training’, ‘validation’, and ‘test’ sets.⁴⁵ Another 13-member dataset from Chen *et al.*¹² was used in a second validation process discussed below.

Measure of model accuracy

In this work, the training set was used to generate ANNs with varying weights and biases. The validation set was used to estimate the error of ANN models and check the stopping criteria. For example, the ANN models stop when the number of iterations (epochs) reaches a maximum, the value of performance indicator on training set reaches the target, and the number of continuous iterations that have increased performance of validation set reaches the predefined validation check time. The test set was used to evaluate the performance of ANNs. In this study, the error of ANN on a dataset was calculated by the mean square error (MSE, given by Eqn (6)), a commonly used cost function for a LM-BP algorithm. The performances of ANNs were measured with other performance indicators such as correlation coefficient (R^2 , given by Eqn (7)), and mean average percentage error (MAPE, given by Eqn (8)). The MSE, R^2 and MAPE are expressed as:

$$MSE = \frac{1}{n} \sum_{i=1}^n (y_{i,\text{exp}} - y_{i,\text{sim}})^2 \quad (6)$$

$$R^2 = 1 - \frac{\sum_{i=1}^n (y_{i,\text{exp}} - y_{i,\text{sim}})^2}{\sum_{i=1}^n (y_{i,\text{exp}} - y_{\text{avg}})^2} \quad (7)$$

$$MAPE = \frac{1}{n} \sum_{i=1}^n \left| \frac{y_{i,\text{exp}} - y_{i,\text{sim}}}{y_{i,\text{exp}}} \right| \times 100\% \quad (8)$$

where $y_{i,\text{exp}}$ is the value of the i th experimental data, $y_{i,\text{sim}}$ is the value of the i th ANN predicted data, y_{avg} is the average value of the experimental data, and n is the size of dataset.

In this work 70%, 15%, and 15% of the 155 samples were randomly allocated to the training, validation, and test sets. Thirteen independent data samples that were not included in the previous three sets were used to test the model in a second validation and test for overfitting.^{12,22} The ANN training was conducted using MATLAB R2017a Neural Network Toolbox. The stopping criteria were 1000 epochs as the maximum number of iterations, 10^{-4} as the target MSE, and 20 times as the predefined validation check time.

Contribution analysis

The Garson equation (Eqn (9)) was used in this work to understand the relative importance of each input parameter:⁴⁶

$$I_i = \frac{\sum_{j=1}^n \left(\frac{|w_{ij}|}{\sum_{i=1}^m |w_{ij}|} * |w_{jk}| \right)}{\sum_{i=1}^m \left(\sum_{j=1}^n \left(\frac{|w_{ij}|}{\sum_{i=1}^m |w_{ij}|} * |w_{jk}| \right) \right)} \quad (9)$$

where I_i represents the relative importance of the i th input parameter of the ANN model, n represents the number of neurons in the hidden layer, m represents the number of input variables, w_{ij} represents the weight between the i th neuron in the input layer and the j th neuron in the hidden layer, and w_{jk} represents the weight between the j th neuron in the hidden layer and the k th neuron in the output layer.

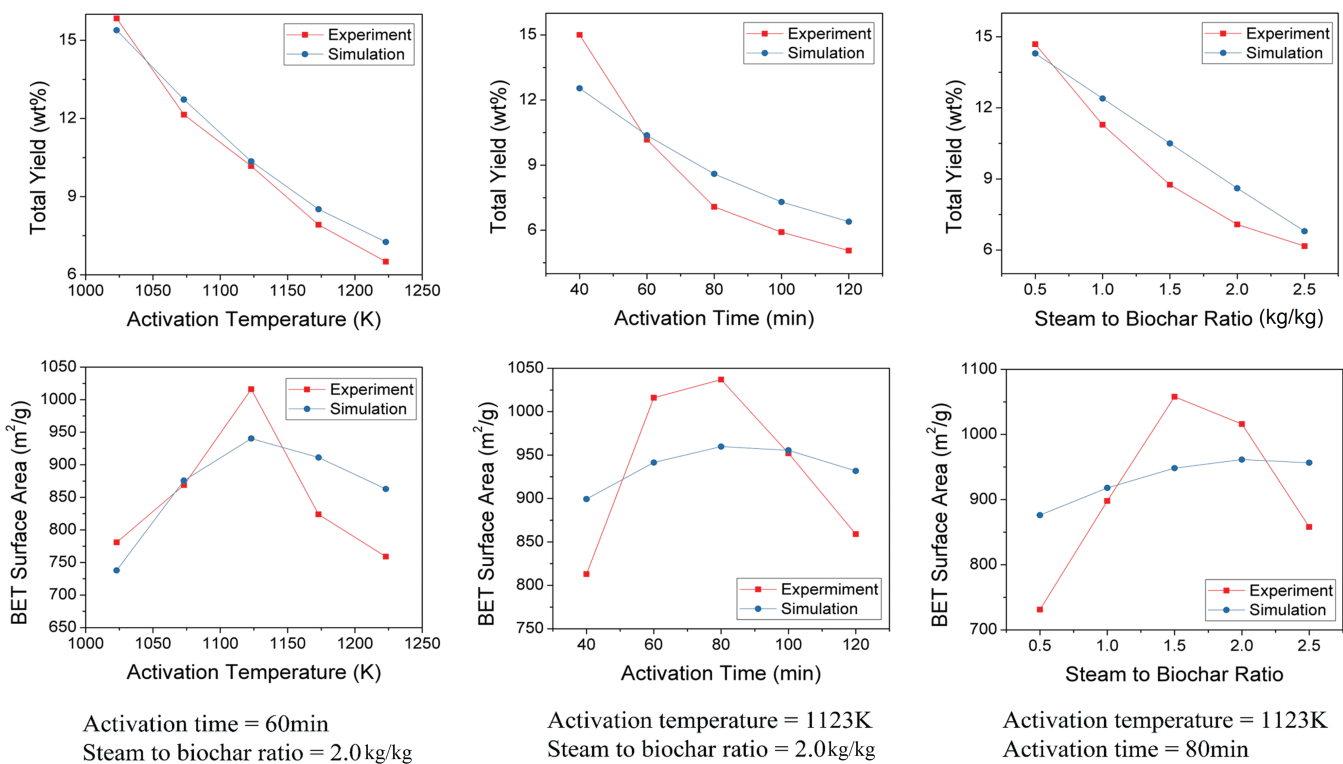
Results and discussion

ANNs and validation

Table 1 shows performance indicators for the ANN models, using different parameters. Overall the ANN models show high accuracy ($R^2 > 0.92$) and low MSE (< 0.01). The

Table 1. Performance of ANN models.

Scenarios	R ²			MSE			MAPE		
	1	2	3	1	2	3	1	2	3
<i>ANN models for total AC yield</i>									
Training	0.983	0.994	0.996	0.0016	0.0004	0.0004	0.0623	0.0348	0.0286
Validation	0.930	0.924	0.951	0.0086	0.0099	0.0051	0.2497	0.2588	0.1140
Testing	0.960	0.962	0.931	0.0034	0.0041	0.0050	0.1393	0.1654	0.1595
Overall	0.970	0.971	0.982	0.0030	0.0024	0.0019	0.1028	0.0879	0.0618
<i>ANN models for BET surface area</i>									
Training	0.973	0.977	0.945	0.0031	0.0016	0.0037	0.1095	0.0734	0.0899
Validation	0.923	0.905	0.966	0.0041	0.0052	0.0018	0.1234	0.1343	0.0788
Testing	0.940	0.930	0.922	0.0016	0.0031	0.0034	0.0720	0.1090	0.1311
Overall	0.961	0.962	0.944	0.0030	0.0024	0.0034	0.1059	0.0881	0.0945
Scenario 1: Proximate analysis + carbonization conditions + activation conditions (8 input variables)									
Scenario 2: Ultimate analysis + carbonization conditions + activation conditions (8 input variables)									
Scenario 3: Proximate analysis + ultimate analysis + carbonization conditions + activation conditions (11 Input variables)									

**Figure 2. The extra validation comparing the experimental data from Chen et al. and prediction of ANN models in scenario 1 (proximate analysis data only for biomass composition).**

low MAPE value suggests the high robustness of the ANN models.

As discussed in the previous section, three scenarios were developed to investigate the impacts of using different data as inputs for the biomass composition. Scenario 1 is based only on proximate analysis data, scenario 2 is

based only on the ultimate analysis, and scenario 3 uses both sets of data. Based on the performance indicators shown in Table 1, there were no significant differences in using different biomass characterization data for ANN training to achieve high accuracy. However, in the extra validation step using only the data from Chen *et al.*¹², the

ANN models trained in three scenarios demonstrate different capabilities in predicting Y_T and S_{BET} for AC derived from a biomass feedstock that was not in the original training datasets. This capability is critical if this ANN approach is to serve as an effective tool to enhance biomass R&D decision making, such as screening biomass feedstock for high Y_T and S_{BET} , or preselecting operational conditions for experiments.

In the work by Chen *et al.*, the carbonization temperature and carbonization time were fixed at 600 °C and 10 min. The activation conditions were varied between 750 and 950 °C for activation temperature, 40–120 min for activation time, and 0.5–2.5 kg kg⁻¹ for steam-to-biochar ratio. Activation temperature, activation time, and steam-to-biochar ratio were varied based on three experimental scenarios in their study, including varied activation temperature with fixed activation time (60 min) and steam-to-biochar ratio (2 kg kg⁻¹); varied activation time with fixed activation temperature (1123 K) and steam-to-biochar ratio (2 kg kg⁻¹); and varied steam-to-biochar ratio with fixed activation temperature (1123 K) and activation time (80 min). Figure 2 shows validation results for the Chen *et al.* data, predicted from the ANN models developed for scenario 1, i.e., proximate analysis data only. Figure 2 shows good alignment (error% < 30%) between the ANN-

predicted response and the experimental data for Y_T , and a more modest correlation between the predict and measured S_{BET} . Overall, these results demonstrate the potential for the ANN models to predict the Y_T and S_{BET} area for AC over a wide variety of processing conditions.

Figure 3 shows the results for using the ANN models developed from ultimate analysis data (scenario 2) to predict the Y_T and S_{BET} . Similar to Fig. 2, there was a good alignment between simulated and experimental results. However, the nonlinear relationship between steam to biochar ratio and S_{BET} was not captured in this simulation, where S_{BET} decreased then reached a plateau as the steam-to-biochar ratio increased. One possible explanation for the difference could be that the impacts of steam on S_{BET} depend on diffusion rate and porosity of materials,⁴⁷ which are significantly affected by the physical property of biomass feedstock such as fixed carbon and volatile matters.⁴⁸ Such properties are commonly measured by proximate analysis and are not included in the training datasets in scenario 2.

Figure 4 shows the extra validation results for ANN models developed using both ultimate and proximate analysis data as inputs for the ANN model in scenario 3. With this combined set of input data, there is a strong correlation between predicted and experimental Y_T across a

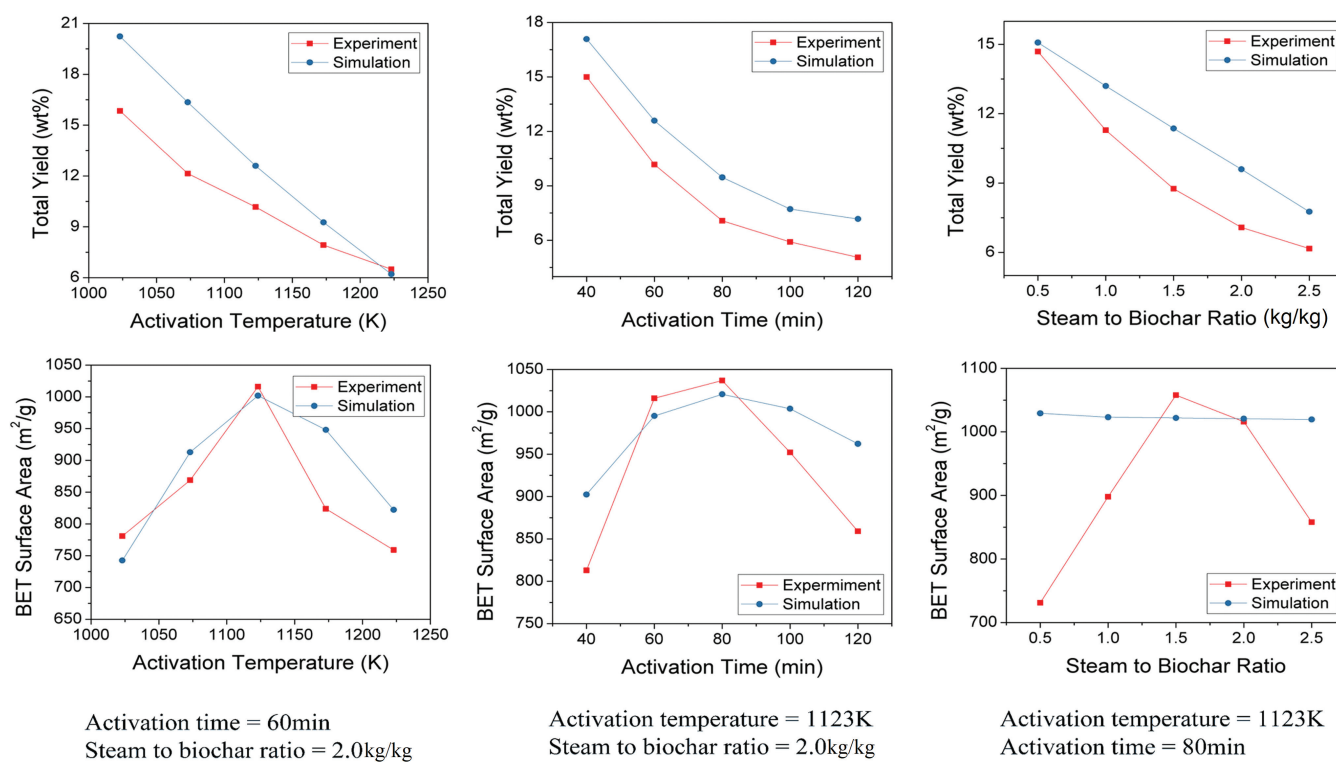


Figure 3. The extra validation comparing the experimental data from Chen *et al.* and prediction of ANN models in scenario 2 (ultimate analysis data only for biomass composition).

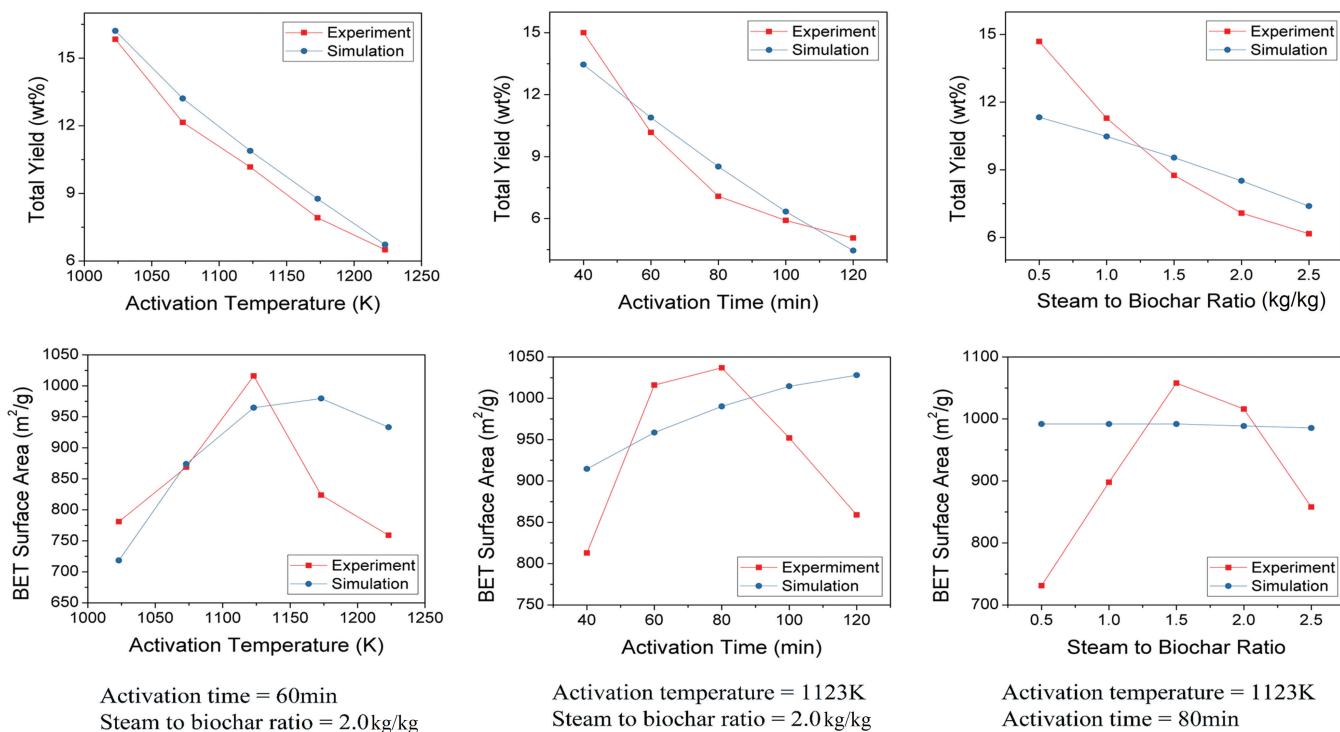


Figure 4. The extra validation comparing the experimental data from Chen et al. and prediction of ANN models in scenario 3 (mixed proximate analysis and ultimate analysis data for biomass composition).

Table 2 Weights and biases used in the optimal ANN to predict total yield of AC (Scenario 2)

Neuron	Hidden layer parameters									Output layer parameters	
	W_{X_C}	W_{X_H}	W_{X_O}	W_{T_C}	W_{t_C}	W_{T_A}	W_{t_A}	$W_{S/C}$	θ	w	
1	-0.0742	1.0628	0.8561	-0.0275	1.0145	0.7989	-0.0839	-0.5489	-2.8226	1.8163	
2	-0.7223	-1.6136	-0.6745	-0.7017	-0.9091	0.4877	0.4566	0.1104	1.1465	0.6195	
3	0.7448	-1.0010	0.1582	0.8094	-0.2485	-1.0584	-0.4159	0.4894	-1.6234	0.0331	
4	-0.0147	1.0750	0.0861	1.9091	1.6131	0.6907	0.4144	0.9707	1.5388	-1.3406	
5	0.4706	-1.2494	0.8894	-0.6711	1.0445	0.7174	0.3334	-0.8871	-0.9298	-0.9010	
6	-1.5042	-0.2274	1.1439	-0.7740	0.3822	-0.6101	1.2652	0.8849	1.5639	-0.8990	
7	1.1938	0.9151	-1.4133	-0.1249	0.8729	-0.5116	0.6141	0.1907	0.2054	2.2368	
8	-1.6905	-0.4474	-0.0631	0.4756	1.3511	0.8524	0.5638	0.7676	1.1947	1.0206	
9	-0.0451	-0.2637	-2.4432	0.4937	-0.4654	0.8219	0.8566	1.0260	0.8949	-1.8249	
10	0.3962	0.8079	-0.1022	-1.8736	-0.7704	0.7291	2.0603	-1.0437	-0.8576	-1.2426	
11	-0.7899	0.5166	-0.3253	-0.2001	-1.6908	-0.2136	0.0312	1.6886	1.5377	0.9721	
12	-0.3573	1.0907	1.8578	1.1435	0.4905	1.0596	0.4662	-0.0616	0.7925	0.9797	
13	-0.4320	0.3750	-0.9786	-1.1292	0.4208	-0.0629	-1.9899	-1.0493	-0.8125	-0.8337	
14	2.3666	-0.5809	-0.7541	-0.8578	-0.6110	0.7934	-1.0628	0.0321	0.9637	1.0458	
15	-0.0237	0.6783	-0.8110	0.8647	0.2639	0.9789	0.2807	1.2243	-1.5851	-0.7498	
16	-0.0527	2.8577	-0.6923	-0.7083	0.1741	0.9953	-1.3520	0.5236	-2.0648	-1.1690	
17	-0.9797	-0.5618	-0.5433	-1.3340	-0.1443	0.4682	-0.3790	-1.0921	-2.1756	1.0441	

w_x : Weight from input layer neuron x to the neuron in hidden layer; w : Weight from neuron in hidden layer to output layer; θ : Bias; X_C : Carbon content; X_H : Hydrogen content; X_O : Oxygen content; T_C : Carbonization temperature; t_C : Carbonization time; T_A : Activation temperature; t_A : Activation time; S/C : Steam to biochar ratio

Table 3 Weights and biases used in the optimal ANN to predict BET surface area of AC (Scenario 1)

Neuron	Hidden layer parameters								Output layer parameters	
	W_{Fc}	W_{VM}	W_{Ash}	W_{T_C}	W_{t_c}	W_{T_A}	W_{t_A}	$W_{S/C}$	θ	w
1	-0.3026	0.7846	-1.2561	-0.2274	0.9010	1.4649	0.4805	-0.2189	-1.8902	0.2227
2	-0.2845	1.2532	0.0821	0.6226	0.3469	1.9592	-0.5301	0.5390	-1.6346	-0.7958
3	0.8285	1.1161	0.2991	0.0022	1.3017	0.5903	-0.7460	1.4154	-1.3659	0.7321
4	1.0088	-0.1808	0.2196	0.9442	-0.7106	0.1320	1.0556	-0.1574	-1.5218	-0.1641
5	-0.3422	0.7568	-0.8105	0.5623	0.2240	-1.1715	-0.6537	1.8734	1.0850	0.6307
6	-0.6473	-0.6177	-0.8071	-1.1001	0.3922	-0.2106	-0.2179	1.0374	0.9990	0.4637
7	-0.4855	0.5422	1.3458	-0.4587	-0.4231	-0.9753	-0.3769	0.6788	0.4398	0.1568
8	-1.2994	0.2391	0.1549	-0.1736	0.7105	0.0001	1.6304	0.0126	0.4417	-0.2693
9	0.0008	-0.4089	0.7066	-0.5899	0.8827	1.0616	-0.7257	-0.8674	0.2647	0.2191
10	-0.7427	0.6484	-0.7382	0.6259	0.7459	-0.3752	-0.2321	0.0454	-0.2743	-0.8738
11	-0.1532	0.1109	1.1493	0.1956	-1.1429	0.4284	0.6119	1.4019	0.3527	-0.6875
12	-0.1328	1.0411	1.0762	0.2352	1.0244	-0.4504	-0.3545	-0.4759	-0.4867	-0.0133
13	-0.0783	0.1685	0.2050	0.1830	-0.1837	-0.4522	-0.7170	2.8178	1.0840	-1.5516
14	0.8809	-0.0080	1.2365	-0.9509	-0.3330	-1.2400	0.7302	-1.4684	0.8752	-0.8627
15	-1.0913	-0.9906	-1.5273	1.2076	-0.4000	-0.4897	0.0528	1.3480	-0.6425	1.2990
16	0.1535	-0.5642	0.3985	0.8162	-0.8080	0.7277	-0.2164	-0.5318	-1.4683	0.3434
17	-0.3730	-0.7280	-0.8319	-0.1069	0.4567	-0.4997	-1.1399	-0.5615	-1.6784	-1.0034
18	0.7224	-0.6806	-1.1290	-0.9071	0.0372	-0.6858	0.2993	0.7401	1.7582	0.4086
19	0.5989	0.4537	-0.5317	-1.1371	-0.4728	-1.0339	-1.2097	0.3711	1.9283	-0.7092

w_x : Weight from input layer neuron x to the neuron in hidden layer; w : Weight from neuron in hidden layer to output layer; θ : Bias; FC: Fixed carbon; VM: Volatile matters; Ash: Ash content; T_C : Carbonization temperature; t_c : Carbonization time; T_A : Activation temperature; t_A : Activation time; S/C: Steam to biochar ratio

range of processing conditions. However, the correlations for the S_{BET} are poor. This phenomenon could be caused by overfitting where too many variables were provided while the dataset size was not increased. Thus, the ANN models were too complicated to reveal the underlying relationships of new data — in this case, new biomass that was not covered in the training datasets. Overfitting commonly occurs for large models that have many variables. According to May *et al.*,⁴⁹ one strategy is to increase the size of datasets. May *et al.*⁴⁹ demonstrated that the dataset size of an ANN model with ten and more input variables should be 20 times larger than one with eight input variables. For scenario 3 in this study, the dataset needs to be significantly expanded to improve the ANN model, which is not feasible due to lack of data availability but could be achieved in the future when more data are available. Another strategy is to reduce the complexity of ANN — in other words, to reduce the number of input variables,⁵⁰ which is reflected through the three scenarios in this

study. Scenarios 1 and 2 have fewer input variables (or say less complexity with eight input variables) than scenario 3 (11 input variables).

In all three scenarios (Figs 2–4) the ANN models predict Y_T better than S_{BET} . One explanation is the differences in the anatomical and macromolecular morphology of the different biomass samples included in the original training set. There are significant anatomical differences between dense biomass materials such as nut shells, and relatively porous wood biomass with its open structure of fiber lumens and vessels. Even within a single class of material such as wood there are large differences in density, the chemical structure of lignin and hemicelluloses, the diameter of fiber lumens, and interconnections of ray cells. There will also be significant differences between biomass sources related to the detailed macromolecular-level organization of the three dominant biomass structural components – cellulose, hemicellulose, and lignin. All these factors will lead to different chemical reactions, and

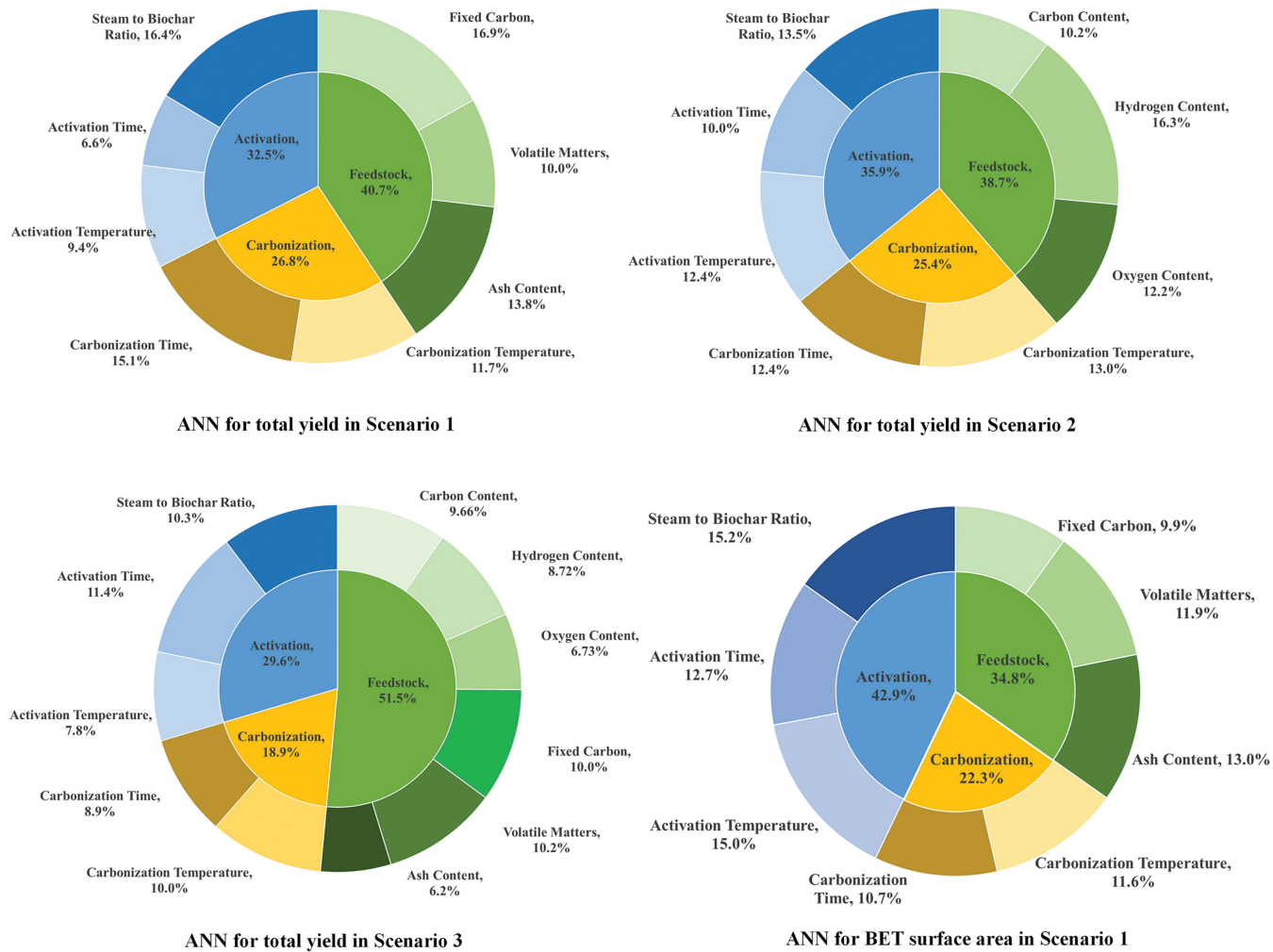


Figure 5. Relative importance of different variables in the ANN models for total yield and BET surface area.

differences in the formation microcracks, that can allow gases and vapors to escape the residual solid as the AC forms. Finally, while the ash content is included as a input for the proximate analysis, there are well known catalytic effects of alkaline earth elements on the decomposition of cellulose and hemicelluloses.^{51,52} The total ash content is thus not the best indicator for the effects of minerals on biomass thermal decomposition reactions.

The weights (w) and biases (θ) generated by the best performing ANN models are summarized in Tables 2 and 3 (scenario 2 for Y_T prediction, $R^2 = 0.962$ for the testing set, and scenario 1 for S_{BET} , $R^2 = 0.940$ for the testing set, prediction based on the highest R^2 and alignment with independent experiment data in the extra validation step). The ANN models presented in this work can be fully reproduced by using the data shown in Tables 2 and 3, and the predefined ANN structure as described in the artificial neural network section above.

These models can be used for biomass screening, and process simulation and optimization for AC production. For example, researchers developing process simulation models of AC production in Aspen Plus, where Y_T is one of the critical inputs,²⁶ can use these models to predict Y_T . This prediction can provide significant savings of time and money, related to having to make a number of experimental runs with multiple sources of biomass.

Relative importance of input parameters

The relative importance of each input parameters for Y_T and S_{BET} is quantified with the Garson equation (Eqn (9)) and shown in Fig. 5. Because all three scenarios show good alignment and reasonable accuracy in predicting Y_T , the results of all three scenarios for Y_T are included. As the ANN models in scenario 2 and scenario 3 cannot reflect the nonlinear relationship between activation operations and

S_{BET} , Fig. 5 only includes the result for the S_{BET} prediction in scenario 1.

Regarding the prediction of Y_T , the results in all scenarios reveal the relative importance of input parameters in descending order: feedstock properties, activation conditions, and carbonization conditions. For the S_{BET} , the activation conditions have the largest impact, followed by feedstock (proximate analysis), and carbonization conditions.

The relative importance of variables in this study can be used to improve the design and operation of the AC production process. More parameters (e.g., particle size distribution, anatomical features or detailed ash composition of biomass, and the heating rate of carbonization or activation) could be included in future work to predict other performance indicators (e.g., energy consumption or environmental footprints). Data availability and quality will be the challenges. For example, during data collection and cleaning for this work, the authors found a number of papers that did not report steam use and final Y_T . The authors also observed different terminology and calculation methods for the same parameter in different papers. To expand the datasets of this work and advance ANN models for AC property prediction or other applications, developing and encouraging standardization of terminology, data reporting, and documentation across academic communities and related research areas will be the key.

Conclusions

The ANN models show high accuracy and alignment with the experimental data for Y_T . For the S_{BET} , the ANN models using proximate analysis data for biomass composition show the best alignment with the experimental data. The contribution analysis shows the large impacts of activation conditions and feedstock properties, indicating the importance of optimizing raw materials and activation conditions. The ANN models can be a powerful tool for feedstock selection and process design, as well as to generate Y_T and S_{BET} data that are needed for process simulation and assessment.

Acknowledgements

This work was supported by the Department of Forest Biomaterials at North Carolina State University.

References

- Mohammad-Khah A and Ansari R, Activated charcoal: Preparation, characterization and applications: A review article. *Int J Chemtech Res* **1**(4):859–864 (2009).
- Dias JM, Alvim-Ferraz MCM, Almeida MF, Rivera-Utrilla J and Sánchez-Polo M, Waste materials for activated carbon preparation and its use in aqueous-phase treatment: A review. *J Environ Manage* **85**(4):833–846 (2007).
- Tan X, Liu S, Liu Y, Gu Y, Zeng G, Hu X et al., Biochar as potential sustainable precursors for activated carbon production: Multiple applications in environmental protection and energy storage. *Bioresour Technol* **227**:359–372 (2017).
- Arena N, Lee J and Clift R, Life cycle Assessment of activated carbon production from coconut shells. *J Clean Prod* **125**:68–77 (2016).
- Adilla Rashidi N and Yusup S, A review on recent technological advancement in the activated carbon production from oil palm wastes. *Chem Eng J* **314**:277–290 (2016).
- González JF, Román S, Encinar JM and Martínez G, Pyrolysis of various biomass residues and char utilization for the production of activated carbons. *J Anal Appl Pyrolysis* **85**(1–2):134–141 (2009).
- Schröder E, Thomauske K, Weber C, Hornung A and Tumiatti V, Experiments on the generation of activated carbon from biomass. *J Anal Appl Pyrolysis* **79**(1–2):106–111 (2007).
- Yeganeh MM, Kaghazchi T and Soleimani M, Effect of raw materials on properties of activated carbons. *Chem Eng Technol* **29**(10):1247–1251 (2006).
- Soleimani M and Kaghazchi T, Agricultural waste conversion to activated carbon by chemical activation with phosphoric acid. *Chem Eng Technol* **30**(5):649–654 (2007).
- Aworn A, Thiravetyan P and Nakbanpote W, Preparation and characteristics of agricultural waste activated carbon by physical activation having micro- and mesopores. *J Anal Appl Pyrolysis* **82**(2):279–285 (2008).
- Li W, Yang K, Peng J, Zhang L, Guo S and Xia H, Effects of carbonization temperatures on characteristics of porosity in coconut shell chars and activated carbons derived from carbonized coconut shell chars. *Ind Crops Prod* **28**(2):190–198 (2008).
- Chen D, Chen X, Sun J, Zheng Z and Fu K, Pyrolysis poly-generation of pine nut shell: Quality of pyrolysis products and study on the preparation of activated carbon from biochar. *Bioresour Technol* **216**:629–636 (2016).
- Rajapaksha AU, Vithanage M, Lee SS, Seo DC, Tsang DCW and Ok YS, Steam activation of biochars facilitates kinetics and pH-resilience of sulfamethazine sorption. *J Soils Sediments* **16**(3):889–895 (2016).
- Zhang YJ, Xing ZJ, Duan ZK, Li M and Wang Y, Effects of steam activation on the pore structure and surface chemistry of activated carbon derived from bamboo waste. *Appl Surf Sci* **315**(1):279–286 (2014).
- Román S, González JF, González-García CM and Zamora F, Control of pore development during CO_2 and steam activation of olive stones. *Fuel Process Technol* **89**(8):715–720 (2008).
- Azargohar R and Dalai AK, Steam and KOH activation of biochar: Experimental and modeling studies. *Microporous Mesoporous Mater* **110**(2–3):413–421 (2008).
- Azargohar R and Dalai AK, Production of activated carbon from Luscar char: Experimental and modeling studies. *Microporous Mesoporous Mater* **85**(3):219–225 (2005).
- Arami-Niya A, Daud WMAW, Mjalli FS, Abnisa F and Shafeeyan MS, Production of microporous palm shell based activated carbon for methane adsorption: Modeling and optimization using response surface methodology. *Chem Eng Res Des* (2012) **90**(6):776–784.

19. Ghani ZA, Yusoff MS, Zaman NQ, Zamri MFMA and Andas J, Optimization of preparation conditions for activated carbon from banana pseudo-stem using response surface methodology on removal of color and COD from landfill leachate. *Waste Manag* **62**:177–187 (2017).
20. Zhong ZY, Yang Q, Li XM, Luo K, Liu Y and Zeng GM, Preparation of peanut hull-based activated carbon by microwave-induced phosphoric acid activation and its application in Remazol Brilliant Blue R adsorption. *Ind Crops Prod* **37**(1):178–185 (2012).
21. Jiang W, Xing X, Li S, Zhang X and Wang W, Synthesis, characterization and machine learning based performance prediction of straw activated carbon. *J Clean Prod* **212**:1210–1223 (2019).
22. Sunphorka S, Chalermsinsuwan B and Piumsomboon P, Artificial neural network model for the prediction of kinetic parameters of biomass pyrolysis from its constituents. *Fuel* **193**:142–158 (2017).
23. Buratti C, Barbanera M and Palladino D, An original tool for checking energy performance and certification of buildings by means of Artificial Neural Networks. *Appl Energy* **120**:125–132 (2014).
24. Sánchez RJ, Fernández MB and Nolasco SM, Artificial neural network model for the kinetics of canola oil extraction for different seed samples and pretreatments. *J Food Process Eng* **41**(1):1–7 (2018).
25. Sun Y, Liu L, Wang Q, Yang X and Tu X, Pyrolysis products from industrial waste biomass based on a neural network model. *J Anal Appl Pyrolysis* **120**:94–102 (2016).
26. Hung JJ, The production of activated carbon from coconut shells using pyrolysis and fluidized bed reactors. The University of Arizona, Tucson, Arizona (2012).
27. Ioannidou O and Zabaniotou A, Agricultural residues as precursors for activated carbon production-A review. *Renew Sust Energy Rev* **11**(9):1966–2005 (2007).
28. Willis MJ, Di Massimo C, Montague GA, Tham MT and Morris AJ, Artificial neural networks in process engineering. *IEE Proc D Control Theory Appl* **138**(3):256–266 (1991).
29. Himmelblau DM, Accounts of experiences in the application of artificial neural networks in chemical engineering. *Ind Eng Chem Res* **47**(1):5782–5796 (2008).
30. González-García P, Activated carbon from lignocellulosics precursors: A review of the synthesis methods, characterization techniques and applications. *Renew Sustain Energy Rev* **82**:1393–1414 (2018).
31. Shen J, Zhu S, Liu X, Zhang H and Tan J, The prediction of elemental composition of biomass based on proximate analysis. *Energy Convers Manage* **51**(5):983–987 (2010).
32. Swingle K, Applying Neural Networks: A Practical Guide, 3rd edn. Morgan Kaufman Publishers, Inc., San Francisco, CA (1996).
33. Rafiq M, Bugmann G, and Easterbrook D, Neural network design for engineering applications. *Comput Struct* **79**(17):1541–1552 (2001).
34. Martin TH, Mark HB and Howard BD. *Neural Network Design*, 2nd edn. PWS Publishing Company, Boston, MA (1996).
35. Soleymani AR, Saieen J and Bayat H, Artificial neural networks developed for prediction of dye decolorization efficiency with UV/K₂S₂O₈ process. *Chem Eng J* **170**(1):29–35 (2011).
36. Mohamed Ismail H, Ng HK, Queck CW and Gan S, Artificial neural networks modelling of engine-out responses for a light-duty diesel engine fuelled with biodiesel blends. *Appl Energy* **92**:769–777 (2012).
37. Shokri A, Hatami T and Khamforoush M, Near critical carbon dioxide extraction of Anise (*Pimpinella Anisum L.*) seed: Mathematical and artificial neural network modeling. *J Supercrit Fluids* **58**(1):49–57 (2011).
38. Ghaffari A, Abdollahi H, Khoshayand MR, Bozchalooi IS, Dadgar A and Rafiee-Tehrani M, Performance comparison of neural network training algorithms in modeling of bimodal drug delivery. *Int J Pharm* **327**(1–2):126–138 (2006).
39. Defernez M and Kemsley EK, Avoiding overfitting in the analysis of high-dimensional data with artificial neural networks (ANNs). *Analyst* **124**(11):1675–1681 (1999).
40. Karsoliya S, Approximating number of hidden layer neurons in multiple hidden layer BPNN architecture. *Int J Eng Trends Technol* **3**(6):714–717 (2012).
41. Cheng J, Li QS and Xiao R-c, A new artificial neural network-based response surface method for structural reliability analysis. *Probabilist Eng Mech* **23**(1):51–63 (2008).
42. Zhou Z, *Machine Learning*, 1st edn. Tsinghua University Press, Beijing (2016).
43. Gevrey M, Dimopoulos I and Lek S, Review and comparison of methods to study the contribution of variables in artificial neural network models. *Ecol Model* **160**:249–264 (2003).
44. Barron AR, Complexity regularization with application to artificial neural networks, in *Nonparametric Functional Estimation and Related Topics*, ed. by Roussas G. Springer, Dordrecht, pp. 561–576 (1991).
45. Moré JJ, The Levenberg-Marquardt algorithm: Implementation and theory, in *Numerical Analysis*, ed. by Watson GA. Springer, Berlin, pp. 105–116 (1978).
46. Garson GD, Interpreting neural-network connection weights. *AI Expert* **6**(4):46–51 (1991).
47. Miguel GS, Fowler GD and Sollars CJ, A study of the characteristics of activated carbons produced by steam and carbon dioxide activation of waste tyre rubber. *Carbon N Y* **41**:1009–1016 (2002).
48. Williams PT and Reed AR, Development of activated carbon pore structure via physical and chemical activation of biomass fibre waste. *Biomass Bioenergy* **30**(2):144–152 (2006).
49. May R, Dandy G, and Maier H, Review of input variable selection methods for artificial neural networks. *Methodol Adv Biomed Appl*, ed. by Suzuki K. IntechOpen, pp. 19–44 (2011).
50. Dreiseitl S and Ohno-Machado L, Logistic regression and artificial neural network classification models: A methodology review. *J Biomed Inform* **35**(5–6):352–359 (2002).
51. Mahadevan R, Adhikari S, Shakya R, Wang K, Dayton D, Lehrich M et al., Effect of alkali and alkaline Earth Metals on in-situ catalytic fast pyrolysis of lignocellulosic biomass: A microreactor study. *Energy Fuels* **30**(4):3045–3056 (2016).
52. Arora JS, Chew JW and Mushrif SH, Influence of alkali and alkaline-earth metals on the cleavage of glycosidic bond in biomass pyrolysis: A DFT study using cellobiose as a model compound. *J Phys Chem A* **122**:7646–7658 (2018).



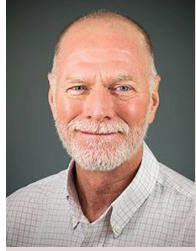
Mochen Liao

Mochen Liao is a PhD student under the direction of Professor Yao in the Department of Forest Biomaterials at North Carolina State University. His research focuses on developing advanced modeling tools for understanding and improving the economic and environmental performance of bioproducts and bioenergy production.



Yuan Yao

Dr Yuan Yao is the assistant professor of sustainability science and engineering in forest biomaterials at North Carolina State University, where she leads the sustainability systems analysis lab. She has been working in the areas of life cycle assessment, process modeling, and optimization for renewable energy systems, sustainable manufacturing, bioenergy, and biochemicals.



Stephen S. Kelley

Dr Stephen S. Kelley is the Reuben B. Robertson Professor in Forest Biomaterials at North Carolina State University, where he also served as department head for 10 years. He has taught classes in sustainable materials, composites, and wood chemistry. He has supervised more than 20 graduate students and postdoctoral associates working on bioenergy, biomaterials, and technical and life-cycle systems analysis.

Artificial neural network based modeling for the prediction of yield and surface area of activated carbon from biomass

Supplementary Information:

Mochen Liao^a, Stephen S Kelley^a, Yuan Yao^{a,*}

^a*Department of Forest Biomaterials, North Carolina State University, 2820 Faucette Drive, Raleigh, 27695, NC, United States*

* Corresponding author: Yuan Yao E-mail: Yuan_Yao@ncsu.edu

Table S1 Experimental data samples used for the training, testing and validation of the ANN model for total yield of AC

Input							Output		Number of Samples		References
Feedstock Properties			Operational Conditions				Y_T	S_{BET} (m ² /g)	Total: 168		References
Proximate Analysis (wt%)		Ultimate Analysis (wt%)	Carbonization (T_C : °C, t_c : min)		Activation (T_A : °C, t_A : min, S/C: kg/kg)				Total: 168		References
X_C	48.72	FC	20.96	T_C	550-800	T_A	800	5.61-23.94	-	15	[1]
X_H	5.78	VM	78.30	t_c	60	t_A	60-270				
X_O	42.53	Ash	0.74			S/C	4.00-20.90				
X_C	44.80-51.30	FC	9.00-16.00	T_C	600	T_A	850	9.90-15.60	601-1080	4	[2]
X_H	6.00-6.60	VM	71.80-80.30	t_c	60	t_A	30				
X_O	41.36-49.09	Ash	0.60-1.40			S/C	1.14				
X_C	48.72	FC	20.96	T_C	400-1000	T_A	900	5.25-19.63	508-1926	16	[3]
X_H	5.78	VM	78.30	t_c	120	t_A	30-120				
X_O	42.53	Ash	0.74			S/C	1.35-5.40				
X_C	47.10	FC	26.60	T_C	450	T_A	550-850	6.32-26.34	459-1210	8	[4]
X_H	6.50	VM	71.70	t_c	60	t_A	60-150				
X_O	42.80	Ash	1.70			S/C	0.81-2.03				
X_C	45.70	FC	15.14	T_C	500	T_A	800	-	322	1	[5]
X_H	5.96	VM	75.75	t_c	60	t_A	45				
X_O	44.98	Ash	0.83			S/C	0.72				
X_C	53.40	FC	21.60	T_C	500	T_A	750-900	9.20-27.37	523-1106	12	[6]
X_H	7.50	VM	67.20	t_c	30	t_A	30-60				
X_O	37.40	Ash	4.40			S/C	0.48-0.96				
X_C	44.80	FC	13.80	T_C	600	T_A	800-900	4.20-12.74	589-1074	6	[7]
X_H	6.00	VM	74.40	t_c	60	t_A	20-60				
X_O	49.09	Ash	1.40			S/C	6.67-20.00				
X_C	38.10-58.60	FC	-	T_C	800	T_A	800	5.96-34.93	-	11	[8]
X_H	5.70-6.50	VM	-	t_c	60	t_A	120				
X_O	30.80-51.20	Ash	-			S/C	5.30-11.16				
X_C	45.10	FC	15.90	T_C	600	T_A	700-900	6.48-18.27	542-1361	7	[9]
X_H	6.00	VM	71.80	t_c	60	t_A	30-120				

X_O	48.60	<i>Ash</i>	1.30		<i>S/C</i>	1.20-4.80				
X_C	48.65	<i>FC</i>	14.47	T_C	600	T_A	700-950			
X_H	5.53	<i>VM</i>	84.24	t_C	120	t_A	67.2-315	8.68	722	6
X_O	44.04	<i>Ash</i>	1.29			<i>S/C</i>	1.13-5.29			[10]
X_C	48.72	<i>FC</i>	20.96	T_C	600	T_A	750-950			
X_H	5.78	<i>VM</i>	78.30	t_C	120	t_A	30-150	3.22-18.54	511-1485	13
X_O	42.53	<i>Ash</i>	0.74			<i>S/C</i>	2.70-7.00			[11]
X_C	48.30	<i>FC</i>	15.80	T_C	500	T_A	850			
X_H	0.50	<i>VM</i>	67.50	t_C	120	t_A	105	24.30	290	1
X_O	44.40	<i>Ash</i>	16.70			<i>S/C</i>	2.98			[12]
X_C	41.20-46.60	<i>FC</i>	12.90-15.80	T_C	450	T_A	800			
X_H	5.90-6.50	<i>VM</i>	74.90-78.70	t_C	60	t_A	240	9.80-21.70	776-877	5
X_O	47.50-52.20	<i>Ash</i>	0.30-1.80			<i>S/C</i>	1.93			[13]
X_C	43.37	<i>FC</i>	16.60	T_C	700	T_A	500-800			
X_H	6.23	<i>VM</i>	82.00	t_C	60	t_A	30-360	3.04-6.33	322-514	9
X_O	49.05	<i>Ash</i>	1.40			<i>S/C</i>	0.21-2.49			[14]
X_C	48.26	<i>FC</i>	19.18	T_C	600	T_A	750-950			
X_H	6.43	<i>VM</i>	80.23	t_C	10	t_A	40-120	5.06-15.84	731-1058	13
X_O	44.08	<i>Ash</i>	0.59			<i>S/C</i>	0.50-2.50			[15]
X_C	53.40-55.00	<i>FC</i>	18.10-27.40	T_C	450	T_A	850-950			
X_H	6.50-7.80	<i>VM</i>	68.50-75.50	t_C	60	t_A	30-120	8.30-27.30	336-1179	12
X_O	31.10-37.90	<i>Ash</i>	2.60-4.90			<i>S/C</i>	0.06-0.31			[16]
X_C	48.60	<i>FC</i>	25.48	T_C	600	T_A	900			
X_H	7.23	<i>VM</i>	60.78	t_C	60	t_A	22	13.32	748	1
X_O	41.10	<i>Ash</i>	3.80			<i>S/C</i>	3.03			[17]
X_C	41.94-66.08	<i>FC</i>	14.90-18.19	T_C	400	T_A	800			
X_H	1.41-6.37	<i>VM</i>	69.30-82.03	t_C	60	t_A	10-240	7.21-30.76	68-947	23
X_O	25.00-51.36	<i>Ash</i>	1.13-15.80			<i>S/C</i>	0.05-1.85			[18]
X_C	52.80-53.50	<i>FC</i>	18.00-22.00	T_C	450	T_A	800			
X_H	6.40-6.90	<i>VM</i>	75.00-76.00	t_C	15	t_A	227-242	12.60-14.60	682-810	3
X_O	36.60-37.60	<i>Ash</i>	2.20-3.10			<i>S/C</i>	1.50			[19]
X_C	45.92	<i>FC</i>	17.90	T_C	600	T_A	850-900			
X_H	6.09	<i>VM</i>	71.70	t_C	30	t_A	30-60	28.00-29.00	1257-1258	2
X_O	47.38	<i>Ash</i>	1.10			<i>S/C</i>	0.06-0.13			[20]

X_C : Carbon content of feedstock; X_H : Hydrogen content of feedstock; X_O : Oxygen content of feedstock; FC : Fixed carbon of feedstock; VM : Volatile matters of feedstock; Ash : Ash content of feedstock; T_C : Carbonization temperature; t_C : Carbonization time; T_A : Activation temperature; t_A : Activation time; S/C : Steam to biochar ratio; Y_T : Total yield of AC; S_{BET} : BET surface area of AC

Reference

1. Cagnon, B., Py, X., Guillot, A., and Stoeckli, F. (2003) The effect of the carbonization/activation procedure on the microporous texture of the subsequent chars and active carbons. *Microporous Mesoporous Mater.*, **57** (3), 273–282.
2. González, J.F., Román, S., Encinar, J.M., and Martínez, G. (2009) Pyrolysis of various biomass residues and char utilization for the production of activated carbons. *J. Anal. Appl. Pyrolysis*, **85** (1–2), 134–141.
3. Li, W., Yang, K., Peng, J., Zhang, L., Guo, S., and Xia, H. (2008) Effects of carbonization temperatures on characteristics of porosity in coconut shell chars and activated carbons derived from carbonized coconut shell chars. *Ind. Crops Prod.*, **28** (2), 190–198.
4. Zhang, Y.J., Xing, Z.J., Duan, Z.K., Li, M., and Wang, Y. (2014) Effects of steam activation on the pore structure and surface chemistry of activated carbon derived from bamboo waste. *Appl. Surf. Sci.*, **315** (1), 279–286.
5. Shim, T., Yoo, J., Ryu, C., Park, Y.K., and Jung, J. (2015) Effect of steam activation of biochar produced from a giant Miscanthus on copper sorption and toxicity. *Bioresour. Technol.*, **197**, 85–90.
6. Demiral, H., Demiral, I., Karabacakoglu, B., and Tümsek, F. (2011) Production of activated carbon from olive bagasse by physical activation. *Chem. Eng. Res. Des.*, **89** (2), 206–213.
7. Román, S., González, J.F., González-García, C.M., and Zamora, F. (2008) Control of pore development during CO₂ and steam activation of olive stones. *Fuel Process. Technol.*, **89** (8), 715–720.
8. Cagnon, B., Py, X., Guillot, A., Stoeckli, F., and Chambat, G. (2009) Contributions of hemicellulose, cellulose and lignin to the mass and the porous properties of chars and steam activated carbons from various lignocellulosic precursors. *Bioresour. Technol.*, **100** (1), 292–298.
9. Gonzalez, J., Gonza, J.F., Roma, S., Gonza, C.M., Ortiz, A.L., and Roma, R. (2009) Porosity Development in Activated Carbons Prepared from Walnut Shells by Carbon Dioxide or Steam Activation Porosity Development in Activated Carbons Prepared from Walnut Shells by Carbon Dioxide or Steam Activation. (August 2015), 7474–7481.
10. Pastor-Villegas, J., and Durán-Valle, C.J. (2002) Pore structure of activated carbons prepared by carbon dioxide and steam activation at different temperatures from extracted rockrose. *Carbon N. Y.*, **40** (3), 397–402.
11. Wang, X.Y., Li, D.X., Yang, B.M., and Li, W. (2012) Textural Characteristics of Coconut Shell-Based Activated Carbons with Steam Activation. *Adv. Mater. Res.*, **608–609**, 366–373.
12. Deiana, C., Granados, D., Venturini, R., Amaya, A., Sergio, M., and Tancredi, N. (2008)

- Activated carbons obtained from rice husk: Influence of leaching on textural parameters. *Ind. Eng. Chem. Res.*, **47** (14), 4754–4757.
- 13. Reed, A.R., and Williams, P.T. (2004) Thermal processing of biomass natural fibre wastes by pyrolysis. *Int. J. Energy Res.*, **28** (2), 131–145.
 - 14. Bouchelta, C., Medjram, M.S., Bertrand, O., and Bellat, J.P. (2008) Preparation and characterization of activated carbon from date stones by physical activation with steam. *J. Anal. Appl. Pyrolysis*, **82** (1), 70–77.
 - 15. Chen, D., Chen, X., Sun, J., Zheng, Z., and Fu, K. (2016) Pyrolysis polygeneration of pine nut shell: Quality of pyrolysis products and study on the preparation of activated carbon from biochar. *Bioresour. Technol.*, **216**, 629–636.
 - 16. Smets, K., De Jong, M., Lupul, I., Gryglewicz, G., Schreurs, S., Carleer, R., and Yperman, J. (2016) Rapeseed and raspberry seed cakes as inexpensive raw materials in the production of activated carbon by physical activation: Effect of activation conditions on textural and phenol adsorption characteristics. *Materials (Basel)*, **9** (7).
 - 17. Xin-hui, D., Srinivasakannan, C., Jin-hui, P., Li-bo, Z., and Zheng-yong, Z. (2011) Comparison of activated carbon prepared from Jatropha hull by conventional heating and microwave heating. *Biomass and Bioenergy*, **35** (9), 3920–3926.
 - 18. Hsi, H.C., Horng, R.S., Pan, T.A., and Lee, S.K. (2011) Preparation of activated carbons from raw and biotreated agricultural residues for removal of volatile organic compounds. *J. Air Waste Manag. Assoc.*, **61** (5), 543–551.
 - 19. Stals, M., Vandewijngaarden, J., Wróbel-iwaniec, I., Gryglewicz, G., Carleer, R., Schreurs, S., and Yperman, J. (2013) Characterization of activated carbons derived from short rotation hardwood pyrolysis char. *J. Anal. Appl. Pyrolysis*, **101**, 199–208.
 - 20. Tsoncheva, T., Mileva, A., Tsyntsarski, B., Paneva, D., Spassova, I., Kovacheva, D., Velinov, N., Karashanova, D., Georgieva, B., and Petrov, N. (2018) Activated carbon from Bulgarian peach stones as a support of catalysts for methanol decomposition. *Biomass and Bioenergy*, **109** (October 2017), 135–146.